SUPPORTING INFORMATION

Remarkable high efficiency of red emitters using Eu(III) ternary complexes

Alena S. Kalyakina[a,b], Valentina V. Utochnikova[b,c], Manuel Zimmer[d], Fabian Dietrich[d], Anna M. Kaczmarek[e], Rik Van Deun[e], Andrey A. Vashchenko[f], Alexander Goloveshkin[g], Martin Nieger[h], Markus Gerhards[d], Ute Schepers[i], Stefan Bräse*[a,i]

a. *Karlsruhe Institute of Technology, Institute of Organic Chemistry, Fritz-Haber-Weg 6, 76131 Karlsruhe, Germany*
b. *Lomonosov Moscow State University, Leninskie Gory, 1, 119991, Moscow, Russia*
c. *SIA Evoled, Puskina iela 1A-24, Riga, LV-1050, Latvia*
d. *Chemistry Department and Research Center Optimas, TU Kaiserslautern, Erwin-Schrödinger-Straße 52, 67663 Kaiserslautern, Germany*
e. *Inorganic and Physical Chemistry Department, Ghent University, Krijgslaan 281-S3, 9000 Gent, Belgium*
f. *P.N. Lebedev Physical Institute, Leninsky prosp. 53, Moscow, 119992, Russia*
g. *A. N. Nesmeyanov Institute of Organoelement Compounds, Vavilova St. 28, INEOS, 119991, Moscow, Russia*
h. *Department of Chemistry, University of Helsinki, P. O. Box 55, FIN-00014, Finland*
i. *Institute of Toxicology and Genetics, Karlsruhe Institute of Technology (KIT), Hermann-von-Helmholtz-Platz 1, 76344 Eggenstein-Leopoldshafen, Germany*

Content

Instrumental and experimental procedures

Materials and methods. All solvents, including deuterated solvents used for NMR analysis ($CDCl_3$, DMSO-d_6), were purchased from SigmaAldrich, ABCR, Fischer and ChemPur and used without further purification. All carboxylic acids HL1-3 as well as axillary ligands Phen and BPhen were purchased from SigmaAldrich. Lanthanide chlorides were purchased from ABCR GmbH.

NMR spectra have been recorded using the following machines:

^{1}H-NMR: Bruker Avance 300 (300 MHz), Bruker Avance 400 (400 MHz), Bruker Avance DRX 500 (500 MHz). The chemical shift δ is expressed in parts per million (ppm) where the residual signal of the solvent has been used as secondary reference: chloroform-d_1 (^{1}H: δ = 7.26 ppm) and dimethyl sulfoxide-d_6 (δ = 2.50 ppm). The spectra were analyzed according to first order.

^{13}C-NMR: Bruker Avance 300 (75 MHz), Bruker Avance 400 (101 MHz), Bruker Avance DRX 500 (126.3 MHz). The chemical shift δ is expressed in parts per million (ppm) where the residual signal of the solvent has been used as secondary reference: chloroform-d_1 (δ = 77.0 ppm) and dimethyl sulfoxide-d_6 (δ = 39.4 ppm). The spectra were ^{1}H-decoupled and characterization of the ^{13}C-NMR-spectra ensued through the DEPT-technique (DEPT = Distortionless Enhancement by Polarization Transfer) and is stated as follows: DEPT: "+" = primary or secondary carbon atoms (positive DEPT-signal), "–" = secondary (negative DEPT-signal), $C_{quart.}$ = quaternary carbon atoms (no DEPT-signal).

^{19}F-NMR: BRUKER Avance 400 (376 MHz). Chemical shifts in ^{19}F NMR spectra were calculated without reference by the instrument.

All spectra were obtained at room temperature. As solvents, products obtained from Eurisotop and Sigma Aldrich were used: chloroform-d_1 and dimethyl sulfoxide-d_6. For central symmetrical signals the midpoint is given, for multiplets the range of the signal region is given. The multiplicities of the signals were abbreviated as follows: s = singlet, d = doublet, t = triplet, q = quartet, hept = heptet, bs = broad singlet, m = multiplet, b = broad (unresolved) and combinations thereof. All coupling constants *J* are stated as modulus in Hertz [Hz].

Elemental Analysis (CHN) measurements were conducted on a Elementar *Vario Micro*. As analytical scale SARTORIUS *M2P* was used. Notation of Carbon (C), Hydrogen (H) and Nitrogen (N) is given in mass percent. Following abbreviations were used: calc. = expected value (calculated); found = value found in analysis.

Infrared spectra (IR)-spectra were recorded on a Bruker Alpha P and a Bruker *IFS 88*. Measurement of the samples was conducted via attenuated total reflection (ATR). The absolute intensity of bands (strength of absorption) was described as follows: vs = very strong (0-10% transmission, T); s = strong (10-40% T); m = middle (40-70% T); w = weak (70-90%); vw = very weak (90-100%). Position of the absorption bands is given as wavenumber $\tilde{\nu}$ with the unit [cm^{-1}].

The **time-resolved FTIR (trFTIR)** experiments were performed with a Bruker VERTEX 80v spectrometer that was operated in step-scan mode. Signal recording and processing was done by a liquid-nitrogen cooled mercury cadmium telluride (MCT) detector (Kolmar Tech., Model KV100-1-B-7/190) with a risetime of 25 ns, connected to a fast preamplifier and a 14-bit transient recorder board (Spectrum Germany, M3I4142, 400 MS/s). For the excitation of the sample a Q-switched Nd:YAG laser (Lumonics HY750, frequency tripled to 355 nm) that generates excitation pulses with a half-width of about 10 ns and a repetition rate of 10 Hz is used. The timing of the laser pulse and the step-scan triggering was performed by a STANFORD RESEARCH SYSYTEMS DG535 delay generator. The UV pump beam was adjusted to have a maximum overlap with the spectrometer's IR probe beam. To avoid backscattering of the UV laser radiation into the detector or interferometer compartment, anti-reflection-coated

germanium filters were placed inside the sample compartment. The 355 nm excitation laser beam was attenuated to ca. 5 mJ/shot at a diameter of about 9 mm. The temporal resolution of the digitization at the 14-bit transient recorder board was set to 100 ns. The step-scan experiment was started 50 µs before the laser (355 nm) reached the sample. Hence, this time was set as zero point in all spectra. A total number of 1248 coadditions at each interferogram point were recorded. The spectral region was limited by undersampling to 0-1975 cm^{-1} with a spectral resolution of 4 cm^{-1} (resulting in 1110 interferogram points). For the prevention of problems by performing a Fourier transformation, an IR longpass filter (cutoff at 1900 cm^{-1}) was used (i.e. no IR intensity outside the measured region should be observed). After every step-scan measurement, it was checked by a (ground state) FTIR spectrum that the sample undergoes no decomposition. *Sample Preparation.* The complex **1a** (approx. 2 mg) was mixed with dry KBr (approx. 200 mg) (stored in a compartment dryer at 70°C) and grinded to a homogenous mixture. This mixture was filled in an evacuable pellet die with a diameter of 13 mm and sintered at a pressure of 0.75 GPa. The concentration of the sample in the pellet has been chosen in a way that the most intense peak at 1610 cm^{-1} had an absorption of ca. 0.65 OD. The sample compartment was evacuated after the sample was fixed in the sample position.

TD-DFT. The crystal structure was used as initial structure for the quantum-chemical calculations. For the optimization, the B3LYP functional of GAUSSIAN 09 is used with the cc-pVDZ basis set for F, C, H, N, and O and the MWB52 ECP for Eu. Frequency calculation is used to demonstrate the existence of a minimum structure where no imaginary frequency is found. Excitations are calculated using TD-DFT with the same functional and basis set. Since the MWB52 ECP is used for Eu, no f-f excitation can be simulated.

Single crystal X-ray diffraction studies were carried out using a BRUKER APEX Duo CCD or Bruker Nonius Kappa CCD diffractometer (ω-scans) at 120 K using Cu-Kα- or Mo-Kα-radiation. All structures were solved by direct methods and then refined least-squarely using isotropic-anisotropic full-matrix approximation against $|F_{hkl}|^2$. For organic compounds as well as for several lanthanide complexes hydrogen atoms were found from difference Fourier synthesis of electron density, while for other structures (mostly the complexes with earlier Ln, such as La, Sm, Eu, Gd, Tb) H-atoms were calculated using H-bonding network analysis both in monomers and in dimers. All hydrogen atoms were refined isotropically using the riding model with $U_{iso}(H)$ parameters equal to 1.2 $U_{eq}(Ci)$, where $U_{eq}(Ci)$ are respectively the equivalent thermal parameters of the atoms to which corresponding H atoms are bonded. For heterometallic complexes coordinates and anisotropic displacement parameters of metal atoms were constrained on each other while their populations were fixed and equal to 0.5. For the crystals determined as twins indexing were performed using CELL_NOW routine, structures were solved and initially refined using only one domain. The calculations performed using OLEX or SHELX ver. 2014/6.

The powder patterns of all studied compounds were measured on a Bruker D8 Avance Vario diffractometer with Ge(111) monochromator in transmission mode between Mylar films or on a Bruker D8 Advance in reflection mode on Si zero-background holder (Bragg-Brentano geometry, variable slits). Both diffractometers were fitted with LynxEye 1D positional-sensitive detector. The indexing performed using the SVD[1] algorithm as implemented in TOPAS 4.2[2] and solved using the Parallel Tempering algorithm as implemented in FOX[3]. The resulting structures were refined and verified using a symmetrized modification of Morse restraints and statistical analysis of bond length distributions at different values of penalty weighting[4]. Still, given the relative complexity of the studied structures, we used periodic DFT calculations to check the refinement results and obtain more reliable complex geometry[5]. The calculation was performed using PW-PBE approach with Grimme correction[6] as implemented in VASP[7–9], with fixed unit cell and 680 eV energy cutoff. The r.m.s deviation of the optimized structures from reasonably restrained geometry as obtained from powder data was 0.16 Å, lower than the cutoff value proposed by van de Streek[9] for the verification of single-crystal structures. The calculation also unambiguously determined the position of hydrogen atoms of the water molecule. The restraints generated from the calculated structure were used to re-refine the powder data, resulting in slight drop in the R_{wp}. The final structure reported, with r.m.s. bond

Δd from restraints of 0.01 Å, demonstrated $R_{wp}/R_{wp}'/R_p/R_p'/R_{Bragg}$ of 1.70/10.14/1.16/11.25/0.5 % and r.m.s deviation from the optimized structure of 0.10 Å.

Photophysics. The steady state and time resolved luminescence measurements were performed on an Edinburgh Instruments FLSP920 spectrometer setup, using a 450 W xenon lamp as the steady state excitation source and a 60 W pulsed xenon lamp as the time resolved excitation source, operating at a pulse frequency of 100 Hz. The emission was detected using a Hamamatsu R928P PMT photomultiplier. The emission spectra were corrected for the detector response curve. Absolute quantum yields (QYs) of the samples were determined using an integrating sphere covered in BENFLEC (provided by Edinburgh Instruments) by averaging of three independent measurements.

The cytotoxicity of the samples was assessed using a MTT assay. To determine the toxic effect of the probes towards HeLa cells, the CellTiter 96® Non-Radioactive Cell Proliferation Assay (PROMEGA) was used. This assay is based on the intracellular reduction of a tetrazolium salt (yellow) into a formazan product (blue), which only takes place in metabolic active cells. The generated formazan is detectable at wavelengths between 630÷750 nm and is a direct measure for the viability of the cells. For this assay, each well of a 96 well plate (CSTAR 3596, 96 Well Cell Culture Cluster, sterile) was seeded with 1×10^4 HeLa cells in 100 µl Dulbecco's modified Eagle's medium (DMEM, high glucose, Gibco) supplemented with 10% fetal calf serum (FCS, PAA), and 1 U/mL Penicillin/Streptomycin at 37 °C, 5% CO_2 and 95% humidity. After 24 h cells were incubated the samples at different concentrations. For each concentration 6 wells were prepared and incubated for 72 h. A set of positive (cells treated with 5 µl of 20% triton) and negative (untreated cells) control wells, as well as the test samples, were treated with 15 µl of the Dye Solution and incubated for 4 h. 100 µl Solubilization Solution/Stop Mix is then added to each well to solubilize the formazan product, according to the manufacturer's manual. After 24 h incubation the absorbance at 595 nm using a 96-well plate reader (ULTRA MICROPLATE READER ELx808, BIOTEK INSTRUMENTS, INC) was measured. Data were averaged and the multiple determination of each substance and concentration made it possible to calculate the standard deviation

Confocal microscopy. Two hours after seeding 1×10^4 HeLa cells per well plate were transferred into 8-well ibiTreat chamber slides (IBIDI, Martinsried, Germany) in 0.2 mL of the medium. After 24 h, cells were treated with the tested compounds at the desired concentrations. After next 24 h the cells were washed and then investigated using confocal microscope LEICA TCS-SPE (DM2500), equipped with ACS APO 63x/1.30 OIL object-glass. Fluorescence excitation was performed by the 488-nm line or 405-nm line of an Ar-ion laser 15%, resolution 8 bit, line average 16, format 1024 × 1024 pixels, 200 Hz. Fluorescence detection took place either in green channel (450–580 nm) or in the red channel (600–750 nm). Additionally, brightfield images were recorded in a third independent channel. The images were recorded and then analyzed using LAS-AF 2.0.2.4647 software.

OLED manufacturing took place in a clean room class 10000 (Lebedev Physical Institute, Moscow, Russia) in a glovebox with argon atmosphere. The substrates were cleaned by ultrasonication in the following media: NaOH aqueous solution, distilled water, acetone and 2-propanol for 16 min each. A 40 nm-thick thin film of poly(3,4-ethylenedioxythiophene):poly(styrenesulfonate) (PEDOT:PSS) hole-injective layer was first deposited. An aqueous solution of PEDOT:PSS (5 mL) was poured onto the preheated (70 °C) patterned ITO glass substrate, after which the substrate was rotated for 60 s at 2000 rpm. Finally, the deposited film was annealed in air at 80 °C for 60 min. As hole-transport layer PVK solution was spin-coated from toluene (c = 5 g/L). The emission layer was spin-coated from toluene solution (c = 5 mM) on the heterostructure. The electron-transport/hole-blocking layer (TPBi) was thermally evaporated (Univex-300, LEYBORD HERAEUS) under a pressure below 106 mm Hg. The thickness (~30 nm) was controlled by a quartz indicator. The contacts were attached to the electrodes, and the device was sealed with epoxy resin (NORLAND OPTICAL ADHESIVE). Electroluminescence spectra were measured on a PICOQUANT time-correlated single photon counting system used as a conventional spectrofluorimeter. Spectral resolution was 4 nm.

Solubility measurements. The solubility of the synthesized compounds was measured as followed. A suspension of each compound in a desired solvent was refluxed during several hours. After cooling down and complete precipitation 5 mL of clear solution was placed in a vessel with a known mass, and the solvent was evaporated to dryness. The mass change of the vessel corresponded to the quantity of the dissolved product in 5 mL of solvent.

General Procedures

General Procedure for the synthesis of water-soluble lanthanide carboxylates (**GP1**)

An excess of concentrated aqueous solution of NH_3 (10.0 equiv.) is added to an aqueous solution of $LnCl_3 \cdot 6H_2O$ (1.0 equiv.) in water (approx. 50 mL per 2.0 mmol of $LnCl_3 \cdot 6H_2O$). The mixture is stirred for 30 min, the precipitate of $Ln(OH)_3$ is centrifuged and washed with water until the pH of the washing solution become neutral. A small excess of freshly prepared $Ln(OH)_3$ is placed into a beaker and the solution of HL (2.7 equiv.) in the acetone-methanol mixture (3:1) is added. The reaction mixture is stirred for 1 h at 60 °C and the unreacted components are separated by filtration followed by the evaporation of the clear solution to dryness. The obtained solid powder of the lanthanide complexes is then recrystallized from water. Subsequent evaporation procedure at 80 °C during 1 h lead to the precipitation of microcrystalline powder of general formula $Ln(L)_3(H_2O)_x$, where x=0-2. The slow evaporation of aqueous solution of corresponding powder at room temperature gives prismatic and needle single crystals with significantly higher water content (x=5-6).

General Procedure for the synthesis of Eu fluorobenzoates ternary complexes (**GP2**)

The solution of auxillary ligand (either 1,10-phenanthroline or bathophenanthroline) (1.0 equiv.) in ethanol is added to a solution of lanthanide carboxylate (1.0 eqiuv.) in ethanol and the reaction mixture is refluxed for 2 h. The reaction mixture is then allowed to cool to room temperature. The precipitate is recovered by filtration, washed with cold ethanol and dried in vacuo.

Characterization of the synthesized compounds

$Eu(L_1)_3(H_2O)$ (HL_1=2-fluorobenzoic acid) (1)

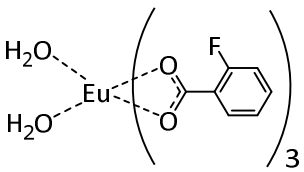

According to **GP1** an excess of concentrated aqueous solution of NH_3 (1.3 mL, 20.0 equiv.) is added to an aqueous solution of 366 mg $LnCl_3 \cdot 6H_2O$ (1.0 mmol, 1.0 equiv.) in 25 mL of water. The mixture is stirred for 30 min, the precipitate of $Ln(OH)_3$ is centrifuged and washed with water until the pH of the washing solution become neutral. A small excess of freshly prepared $Ln(OH)_3$ is placed into a beaker and the solution of 378 mg of 2-fluorobenzoic acid HL_1 (2.7 mmol, 2.7 equiv.) in the 20 mL acetone-methanol mixture (3:1) is added. The reaction mixture is stirred for 1 h at 60 °C and the unreacted components are separated by filtration followed by the evaporation of the clear solution to dryness. The obtained solid powder of the lanthanide complexes is then recrystallized from water. Subsequent evaporation procedure at 80 °C during 1 h lead to the precipitation of microcrystalline powder of general formula $Ln(L_1)_3(H_2O)_2$. Yield 89%.

^{1}H-NMR (300 MHz, DMSO-d_6): δ (ppm) = 7.19 (bs, 1H), 7.02 – 6.42 (m, 3H). – **^{19}F-NMR** (376 MHz, DMSO-d^6): -112.14 (1F, s). – **IR** (ATR): $\tilde{\nu}$ (cm^{-1}) = 3414.1 (vw), 1671.7 (w), 1595.1 (m), 1564.7 (w), 1531.2 (m), 1486.7 (w), 1451.5 (m), 1385.7 (m), 1294.7 (m), 1215.7 (m), 1159.4 (w), 1133.9 (w), 1096.6 (w), 1031.3 (w), 874.0 (w), 843.9 (w), 810.5 (w), 791.7 (w), 750.2 (m), 691.6 (w), 651.3 (m), 566.6 (w), 543.5 (w), 516.6 (w), 450.1 (w), 397.2 (w). – **CHN**: clcd for $Eu(L_1)_3(H_2O)_2$,% C 41.67, H 2.66, found C 41.31, H 2.95.

$Eu(L_2)_3(H_2O)$ (HL_2=2,5-difluorobenzoic acid) (2)

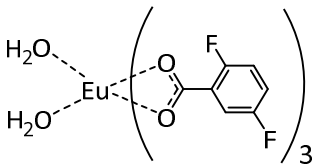

According to **GP1** an excess of concentrated aqueous solution of NH_3 (1.3 mL, 20.0 equiv.) is added to an aqueous solution of 366 mg $LnCl_3 \cdot 6H_2O$ (1.0 mmol, 1.0 equiv.) in 25 mL of water. The mixture is stirred for 30 min, the precipitate of $Ln(OH)_3$ is centrifuged and washed with water until the pH of the washing solution become neutral. A small excess of freshly prepared $Ln(OH)_3$ is placed into a beaker and the solution of 429 mg of 2,5-difluorobenzoic acid HL_2 (2.7 mmol, 2.7 equiv.) in the 20 mL acetone-methanol mixture (3:1) is added. The reaction mixture is stirred for 1 h at 60 °C and the unreacted components are separated by filtration followed by the evaporation of the clear solution to dryness. The obtained solid powder of the lanthanide complexes is then recrystallized from water. Subsequent evaporation procedure at 80 °C during 1 h lead to the precipitation of microcrystalline powder of general formula $Ln(L_2)_3(H_2O)_2$. Yield 91%.

^{1}H-NMR (300 MHz, DMSO-d_6): δ (ppm) =6.93 (1H, m), 6.72 (1H, m), 6.43 (1H, m). – **^{19}F-NMR** (376 MHz, DMSO-d^6): -118.63 (1F, s), -120.57 (1F, d). – **IR** (ATR): $\tilde{\nu}$ (cm^{-1}) = 1600.6 (w), 1540.2 (m), 1486.4 (w), 1432.0 (m), 1374.9 (m), 1244.5 (w), 1191.1 (m), 1121.7 (w), 1083.3 (vw), 944.7 (vw), 890.2 (vw), 822.3 (m), 761.7 (m), 671.9 (w), 584.5 (w), 542.1 (w), 468.5 (w), 416.0 (w). – **CHN**: clcd for $Eu(L_2)_3(H_2O)_2$,% C 38.26, H 1.99, found C 38.63, H 2.42.

$Eu(L_3)_3(H_2O)$ (HL_3=2,4-difluorobenzoic acid) (3)

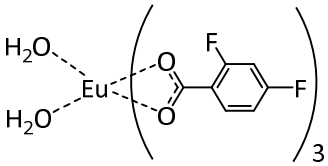

According to **GP1** an excess an excess of concentrated aqueous solution of NH_3 (1.3 mL, 20.0 equiv.) is added to an aqueous solution of 366 mg $LnCl_3 \cdot 6H_2O$ (1 mmol, 1.0 equiv.) in 25 mL of water. The mixture is stirred for 30 min, the precipitate of $Ln(OH)_3$ is centrifuged and washed with water until the pH of the washing solution become neutral. A small excess of freshly prepared $Ln(OH)_3$ is placed into a beaker and the solution of 429 mg of 2-difluorobenzoic acid HL_2 (2.7 mmol, 2.7 equiv.) in the 20 mL acetone-methanol mixture (3:1) is added. The reaction mixture is stirred for 1 h at 60 °C and the unreacted components are separated by filtration followed by the evaporation of the clear solution to dryness. The obtained solid powder of the lanthanide complexes is then recrystallized from water. Subsequent evaporation procedure at 80 °C during 1 h lead to the precipitation of microcrystalline powder of general formula $Ln(L_2)_3(H_2O)_2$. Yield 89%.

^{1}H-NMR (300 MHz, DMSO-d_6): δ (ppm) =6.57 (3H, bs). – **^{19}F-NMR** (376 MHz, DMSO-d^6): -107.02 (2F, bs). – **IR** (ATR): $\tilde{\nu}$ (cm^{-1}) = 3085.7 (vw), 1601.4 (w), 1534.6 (w), 1501.0 (w), 1425.9 (w), 1388.1 (w), 1268.9 (w), 1137.9 (w), 1092.4 (w), 971.3 (w), 849.1 (w), 780.0 (w), 735.3 (w), 684.1 (w), 612.2 (w), 519.9 (vw), 444.8 (vw), 395.9 (w). – **CHN**: clcd for $Eu(L_3)_3(H_2O)_2$,% C 38.26, H 1.99, found C 38.09, H 2.31.

$Eu(L_1)_3$(Phen) (HL_1=2-fluorobenzoic acid, Phen= 1,10-phenanthroline) (1a).

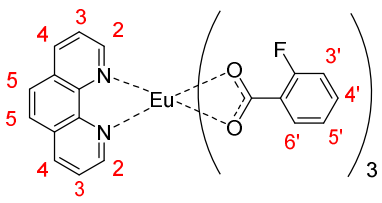

According to **GP2** the solution of 68 mg of 1,10-phenanthroline (0.38 mmol, 1.00 equiv.) in 20 mL of ethanol was added to a solution of 229 mg of tris-europium-2-fluorobenzoate dihydrate **Eu9** (0.38 mmol, 1.00 eqiuv.) in 30 mL of ethanol and the reaction mixture was refluxed for 2 h and then allowed to cool to room temperature. The precipitate was recovered by filtration, washed with cold ethanol and dried in vacuo to afford 230 mg (81%) of a pale pink solid.

^{1}H-NMR (300 MHz, DMSO-d_6): δ (ppm) = 9.10 (bs, 2H, H_2), 8.50 (d, J = 8.0 Hz, 2H, H_4), 8.00 (s, 2H, H_5), 7.77 (bs, 2H, H_3), 7.04 (bs, 3H, H_4), 6.58 (bs, 9H, $H_{6',3',5'}$). – **IR** (ATR): $\tilde{\nu}$ (cm^{-1}) = 1606.9 (m), 1540.6 (w), 1514.6 (w), 1484.9 (w), 1451.3 (w), 1400.2 (m), 1260.1 (vw), 1222.2 (w), 1143.8 (vw), 1093.0 (vw), 1032.7 (vw), 864.3 (w), 853.1 (w), 807.1 (vw), 790.8 (vw), 751.2 (m), 731.8 (m), 722.1 (w), 651.7 (w), 636.9 (vw), 543.2 (vw), 459.4 (vw), 409.4 (vw).

– **CHN**: clcd,% C 52.88, H 2.69, N 3.74, found C 52.97, H 2.61, N 3.82. – **Analytical HPLC** (5–95% acetonitrile + 0.1% TFA in 20 min, detection at 280 nm): t_{Ret} = 9.38 min, 92% purity.

Eu(L_2)$_3$(Phen) (HL_2=2,5-difluorobenzoic acid, Phen= 1,10-phenanthroline) (2a).

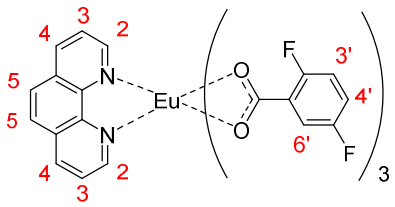

According to **GP2** the solution of 68 mg of 1,10-phenanthroline (0.38 mmol, 1.00 equiv.) in 20 mL of ethanol was added to a solution of 235 mg of tris-europium-2,5-difluorobenzoate dihydrate **Eu7** (0.38 mmol, 1.00 eqiuv.) in 30 mL of ethanol and the reaction mixture was refluxed for 2 h and then allowed to cool to room temperature. The precipitate was recovered by filtration, washed with cold ethanol and dried in vacuo to afford 247 mg (81%) of a pale pink solid.

^{1}H-NMR (300 MHz, DMSO-d_6): δ (ppm) = 9.09 (bs, 2H, H_2), 8.51 (bs, 2H, H_4), 8.01 (s, 2H, H_4), 7.76 (bs, 2H, H_3), 6.92 (s, 3H, $H_{6'}$), 6.66 (s, 3H, $H_{3'}$), 6.20 (s, 3H, $H_{4'}$). – **IR** (ATR): $\tilde{\nu}$ (cm^{-1}) = 1614.0 (m), 1583.1 (m), 1551.1 (m), 1515.7 (w), 1487.7 (m), 1423.2 (m), 1383.0 (s), 1245.0 (m), 1191.9 (m), 1122.0 (w), 941.5 (vw), 890.6 (vw), 853.0 (m), 820.3 (s), 794.1 (w), 756.4 (m), 731.2 (m), 722.1 (m), 697.4 (w), 667.5 (w), 636.9 (vw), 609.5 (vw), 592.6 (vw), 547.3 (vw), 524.6 (w), 468.0 (vw), 415.1 (m). – **CHN**: clcd,% C 49.33, H 2.13, N 3.49, found C 49.37, H 1.98, N 3.58. – **Analytical HPLC** (5–95% acetonitrile + 0.1% TFA in 20 min, detection at 280 nm): t_{Ret} = 9.46 min, 95% purity.

Eu(L_3)$_3$(Phen) (HL_3=2,4-difluorobenzoic acid, Phen= 1,10-phenanthroline) (3a).

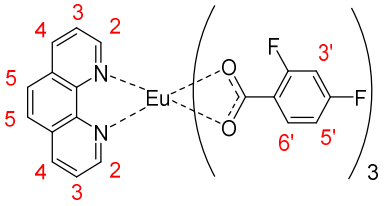

According to **GP2** the solution of 68 mg of 1,10-phenanthroline (0.38 mmol, 1.00 equiv.) in 20 mL of ethanol was added to a solution of 235 mg of tris-europium-2,4-difluorobenzoate dihydrate **Eu6** (0.38 mmol, 1.00 eqiuv.) in 30 mL of ethanol and the reaction mixture was refluxed for 2 h and then allowed to cool to room temperature. The precipitate was recovered by filtration, washed with cold ethanol and dried in vacuo to afford 244 mg (80%) of a pale pink solid.

^{1}H-NMR (300 MHz, DMSO-d_6): δ (ppm) = 9.09 (bs, 2H, H_2), 8.50 (bs, 2H, H_4), 8.00 (s, 2H, H_5), 7.77 (s, 2H, H_3), 6.58 (bs, 9H, $H_{3',4',6'}$). – **IR** (ATR): $\tilde{\nu}$ (cm^{-1}) = 1605.8 (m), 1548.7 (m), 1518.4 (vw), 1502.0 (w), 1424.4 (m), 1390.0 (s), 1268.6 (m), 1135.4 (m), 1091.5 (m), 972.2 (m), 864.5 (w), 846.9 (m), 780.4 (m), 731.1 (m), 700.1 (vw), 620.1 (m), 606.3 (m), 589.6 (m), 520.6 (vw), 458.5 (vw), 417.4 (vw), 390.6 (w). – **CHN**: clcd,% C 49.33, H 2.13, N 3.49, found C 49.42, H 2.01, N 3.61. – **Analytical HPLC** (5–95% acetonitrile + 0.1% TFA in 20 min, detection at 280 nm): t_{Ret} = 9.64 min, 95% purity.

Eu(L_1)$_3$(BPhen) (HL_1=2-fluorobenzoic acid, BPhen= bathophenanthroline) (1b).

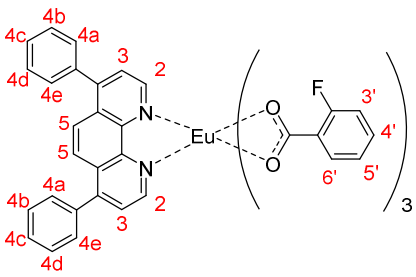

According to **GP2** the solution of 125 mg of bathophenanthroline (0.38 mmol, 1.00 equiv.) in 20 mL of ethanol was added to a solution of 229 mg of tris-europium-2-fluorobenzoate dihydrate **Eu9** (0.38 mmol, 1.00 eqiuv.) in 30 mL of ethanol and the reaction mixture was refluxed for 2 h and then allowed to cool to room temperature. The precipitate was recovered by filtration, washed with cold ethanol and dried in vacuo to afford 264 mg (77%) of a pale pink solid.

^{1}H-NMR (300 MHz, DMSO-d_6): δ (ppm) = 9.17 (d, J = 4.7 Hz, 2H, H_2), 7.86 (s, 2H, H_5), 7.73 (d, J = 4.5 Hz, 2H, H_3), 7.60 (bs, 10H, $H_{4a\text{-}e}$), 7.09 (s, 3H, $H_{6'}$), 6.63 (s, 9H, $H_{3',4',5'}$). – **^{13}C-NMR** (101 MHz, DMSO-d_6): δ (ppm) = 161.1 ($C_{quart.}$, *C*OOH), 149.8 ($C_{quart.}$, C_{Ar}), 132.5 (+, C_{Ar}H), 131.4 ($C_{quart.}$, C_{Ar}), 129.7 (+, C_{Ar}H), 128.9

(+, $C_{Ar}H$), 123.8 (+, $C_{Ar}H$), 123.2 ($C_{quart.}$, C_{Ar}), 114.7 ($C_{quart.}$, C_{Ar}). – **^{19}F-NMR** (377 MHz, DMSO-d_6): δ (ppm) = -116.28 (bs, 1F). – **IR** (ATR): $\tilde{\nu}$ (cm^{-1}) = 1608.1 (m), 1553.4 (m), 1489.1 (vw), 1383.5 (m), 1262.8 (m), 1221.8 (vw), 1148.8 (w), 1092.3 (w), 970.2 (w), 925.0 (vw), 841.3 (m), 765.4 (m), 750.1 (vw), 701.7 (m), 610.8 (m), 543.5 (w), 492.1 (vw), 469.5 (vw). – **CHN**: clcd,% C 59.94, H 3.13, N 3.11, found C 59.11, H 3.27, N 3.09. – **Analytical HPLC** (5–95% acetonitrile + 0.1% TFA in 20 min, detection at 280 nm): t_{Ret} = 10.56 min, 96% purity.

Eu(L_2)$_3$(BPhen) (HL_2=2,5-difluorobenzoic acid, BPhen= bathophenanthroline) (2b).

The solution of 125 mg of bathophenanthroline (0.38 mmol, 1.00 equiv.) in 20 mL of ethanol was added to a solution of 235 mg of tris-europium-2,5-difluorobenzoate dihydrate **Eu7** (0.38 mmol, 1.00 eqiuv.) in 30 mL of ethanol and the reaction mixture was refluxed for 2 h and then allowed to cool to room temperature. The precipitate was recovered by filtration, washed with cold ethanol and dried in vacuo to afford 269 mg (74%) of a pale pink solid.

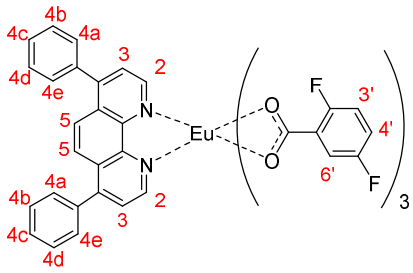

^{1}H-NMR (300 MHz, DMSO-d_6): δ (ppm) = 9.18 (d, J = 4.5 Hz, 2H, H_2), 7.87 (s, 2H, H_5), 7.73 (d, J = 4.5 Hz, 2H, H_3), 7.59 (bs, 10H, $H_{4a\text{-}e}$), 6.95 (s, 9H, $H_{6',4',3'}$). – **^{13}C-NMR** (101 MHz, DMSO-d_6): δ (ppm) = 159.8 ($C_{quart.}$, *C*OOH), 149.5 ($C_{quart.}$, C_{Ar}), 147.4 (+, $C_{Ar}H$), 146.1 ($C_{quart.}$, C_{Ar}), 137.1 ($C_{quart.}$, C_{Ar}), 129.4 (+, $C_{Ar}H$), 128.6 (+, $C_{Ar}H$), 128.5 (+, $C_{Ar}H$), 125.5 ($C_{quart.}$, C_{Ar}), 123.7 (+, $C_{Ar}H$), 123.5 (+, $C_{Ar}H$). – **IR** (ATR): $\tilde{\nu}$ (cm^{-1}) = 1607.6 (m), 1552.2 (m), 1507.4 (vw), 1486.6 (vw), 1380.8 (m), 1269.4 (m), 1189.3 (vw), 1072.4 (w), 1019.2 (w) 970.3 (vw), 923.6 (vw), 841.3 (w), 810.6 (w), 765.2 (m), 749.2 (vw), 701.6 (m), 618.4 (m), 593.2 (w), 541.6 (w), 495.7 (vw), 469.0 (vw). – **CHN**: clcd,% C 56.56, H 2.64, N 2.93, found C 56.51, H 2.77, N 2.84. – **Analytical HPLC** (5–95% acetonitrile + 0.1% TFA in 20 min, detection at 280 nm): t_{Ret} = 10.67 min, 96% purity.

Eu(L_3)$_3$(BPhen) (HL_3=2,4-difluorobenzoic acid, BPhen= bathophenanthroline) (3b).

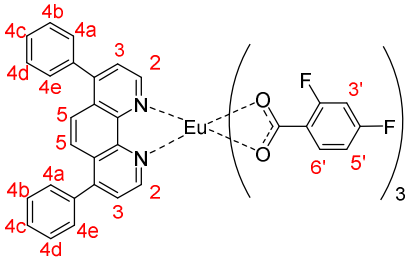

The solution of 125 mg of bathophenanthroline (0.38 mmol, 1.00 equiv.) in 20 mL of ethanol was added to a solution of 235 mg of tris-europium-2,4-difluorobenzoate dihydrate **Eu6** (0.38 mmol, 1.00 eqiuv.) in 30 mL of ethanol and the reaction mixture was refluxed for 2 h and then allowed to cool to room temperature. The precipitate was recovered by filtration, washed with cold ethanol and dried in vacuo to afford 276 mg (76%) of a pale pink solid.

^{1}H-NMR (400 MHz, DMSO-d_6): δ (ppm) = 9.17 (d, J = 4.8 Hz, 2H, H_2), 7.86 (s, 2H, H_5), 7.73 (d, J = 4.5 Hz, 2H, H_3), 7.59 (bs, 10H, $H_{4a\text{-}e}$), 6.61 (s, 9H, $H_{3',5',6'}$). – **^{13}C-NMR** (101 MHz, DMSO-d_6): δ (ppm) = 160.6 ($C_{quart.}$, *C*OOH), 149.66 ($C_{quart.}$, C_{Ar}), 129.73 ($C_{quart.}$, C_{Ar}), 128.90 (+, $C_{Ar}H$), 123.79 (+, $C_{Ar}H$), 110.05 (+, $C_{Ar}H$), 102.21 (+, $C_{Ar}H$), 101.95 (+, $C_{Ar}H$). – **^{19}F-NMR** (377 MHz, DMSO-d_6): δ (ppm) = -111.59 (bs, 2F). – **IR** (ATR): $\tilde{\nu}$ (cm^{-1}) = 1608.1 (m), 1553.8 (m), 1499.3 (vw), 1384.7 (m), 1269.4 (m), 1234.8 (vw), 1138.8 (w), 1091.1 (w), 970.3 (w), 924.1 (vw), 841.3 (m), 784.5 (w), 765.9 (m), 750.2 (vw), 740.0 (w), 701.6 (m), 608.3 (m), 573.5 (w), 543.4 (w), 492.3 (vw), 469.7 (vw). – **CHN**: clcd,% C 56.56, H 2.64, N 2.93, found C 57.02, H 2.71, N 2.96. – **Analytical HPLC** (5–95% acetonitrile + 0.1% TFA in 20 min, detection at 280 nm): t_{Ret} = 10.61 min, 97% purity.

XRD analysis

Single crystals of **1a**, **2a**, were grown from ethanol, **1b** was grown from toluene. The crystal structure of **1a** turned out to be the same as reported previously[10], however, revealing only one type of Eu complex without coordinated solvent molecules (the reported crystal structure contains two dimeric units, one of which contains two coordinated ethanol molecules)[1].

A suitable crystal was selected and placed on a **Bruker APEX-II CCD** diffractometer. The crystal was kept at 120 K during data collection. Using Olex2[11,12], the structure was solved with the XS[12] structure solution program using Direct Methods and refined with the XL[12] refinement package using Least Squares minimization. In the case of **1b** complex, the solvent molecule (toluene) was also presented in a crystal structure, however, being disordered around symmetry center. The toluene were refined with occupancy 0.5 with DFIX bond length restrains, the U_{anis} were equal for all atoms and refined with EADP command.

Both refined structures **1b** and **2a** are centrosymmetric with Eu…Eu distance of 4.042 Å for **2a** and 4.146 Å for **1b**. Though the structures look similar (Figure S1, Figure S2a), their geometry are slightly different (Table S1), which even leads to the different ligand functions. The carboxylic ligand with the chelating-bridging function in the case of **2a** is not chelating in the case of **1b** (denoted with * in the Table S1) and has bidentate bridging function.

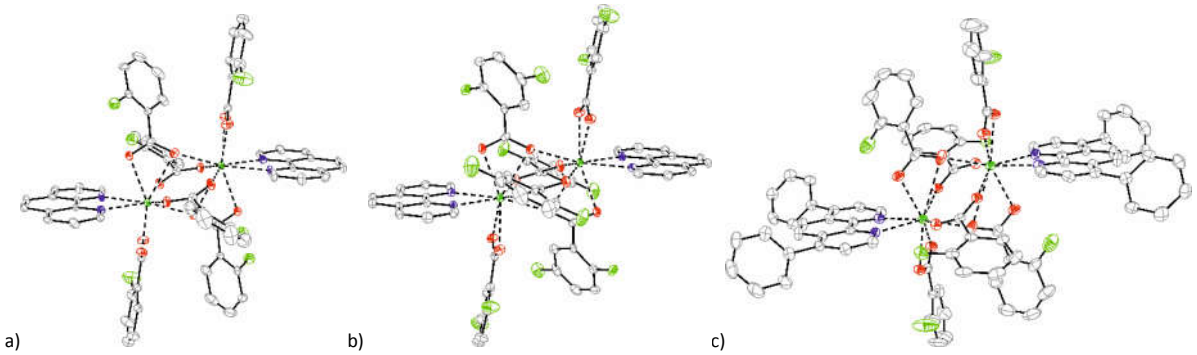

Figure S1 ORTEP drawing of the X-ray structures of the studied complexes with 50% thermal ellipsoids. Atoms assignment: Eu-black, C-blue, O-red, F-green, N-purple. Hydrogen atoms are excluded for clarity.a) **1a** b) **2a** c) **1b**

The complex **2a** is nonacoordinate and acquires a distorted tricapped trigonal prism structure. It is a dimeric molecule with the general formula $Eu_2(L_1)_6(Phen)_2$. Each Eu(III) ion is coordinated by two N atoms of phenanthroline and seven oxygen atoms from the carboxylic ligands. Among six 2,5-fluorobenzoate ligands, two ligands adopt chelating mode, two ligands are bridging and the last two ligands are chelating-bridging. The coordination modes of the ligands are in this case the same as for the structure of ternary complex of samarium benzoate with phenanthroline $Sm_2(bz)_6(Phen)_2$ (CCDC refcode LIXDUR). The complexes in the structure are stabilized by the π–π stacking interactions between phenanthroline moieties. Additionally, phenanthroline molecules are involved in the hydrogen bonding C-H…F with fluoronbenzoate ligand (d=2.465 Å, angle=122.76°), while the same proton also forms hydrogen bond with the oxygen from carboxylic group (d=2.723 Å, angle=144.71°). The neighboring hydrogen atom from phenanthroline moiety also forms weak H-bonds with the carboxylic group (d=2.702 Å, angle=142.28°) as well as an additional short CH…F contacts between phenanthroline and the carboxylic ligand

[1] The crystal data: Chemical formula $C_{66}H_{40}Eu_2F_6N_4O_{12}$, M_r = 1498.94, Crystal system Monoclinic, space group $P2_1/n$, a = 14.3944 (7) Å, b = 13.0642 (7) Å, c = 15.4137 (9) Å, β = 103.999 (2)°, V = 2812.5 (3) Å^3, Z = 2, F(000) = 1480, D_x = 1.770 Mg m^{-3}, Mo Kα radiation, β= 0.71073 Å, μ = 2.30 mm^{-1}, T = 123 K, 0.06 × 0.04 × 0.01 mm

(Figure S2, b). In the case of **1b** the bathophenanthroline moieties are not involved in the stacking interactions However, its phenyl rings from hydrogen bonds C-H…F with one of the fluorobenzoate ligand (d=2.349 Å, angle=167.06°). The molecular units are additionally stabilized by the weak C-H…O interaction between bridging and chelating ligands (d=2.417 Å, angle=138.78°) and C-H…F interaction (d=2.811 Å, angle=98.12°). (Figure S2, c). The refinement data are displayed in the Table S2.

Table S1 . Selected Bond Lengths and Bond Angles of the complexes **1b** and **2a**

Bond	Coordination mode	1b	2a
Eu(1)-O(1)	μ^2-κ^1:κ^2	2.356(3)	2.380(2)
Eu(1)-O(2)	μ^2-κ^1	2.355(3)	2.380(2)
Eu(1)-O(3)	κ^2	2.418(3)	2.470(3)
Eu(1)-O(4)	μ^2-κ^1:κ^2	2.406(3)	2.468(2)
Eu(1)-O(5)	κ^2	2.472(3)	2.457(2)
Eu(1)-O(6)	μ^2-κ^1	2.382(3)	2.361(2)
Eu(1)-O(7)	μ^2-κ^1:κ^2	3.158(4)*	2.708(2)
Eu(1)-N(1)	κ^1	2.557(4)	2.598(3)
Eu(1)-N(2)	κ^1	2.608(4)	2.601(3)

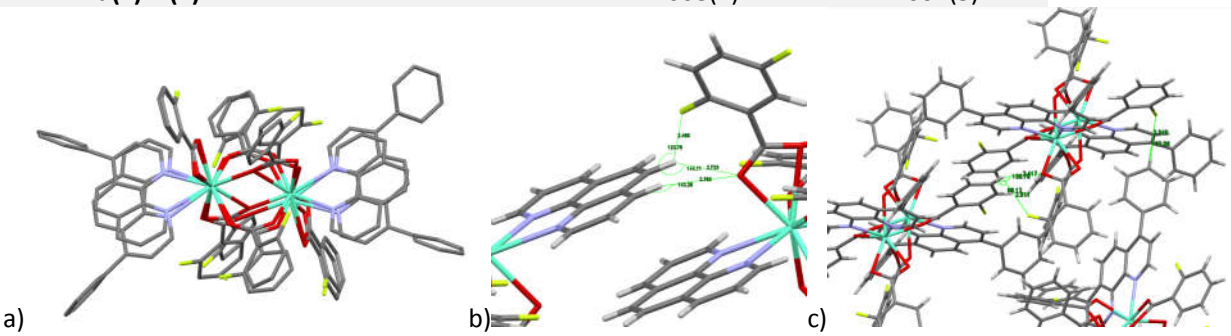

Figure S2 a) the overlay of the structures **2a** and **1b** b) H-bonding in the structure **2a** c) H-bonding in the structure **1b**

Table S2 Single-crystal X-ray diffraction data.

	2a	**1b**
Chemical formula	$C_{66}H_{34}Eu_2F_{12}N_4O_{12}$	$C_{97}H_{64}Eu_2F_6N_4O_{12}$
M_r	1606.89	1895.44
Crystal system, space group	Monoclinic, $P2_1/n$	Monoclinic, $P2_1/c$
Temperature (K)	120	120
***a*, *b*, *c* (Å)**	14.583(2), 13.1391(17), 15.364(2)	11.765(7), 22.391(12), 16.151(9)
α, β, γ (°)	90, 103.713(4), 90	90, 110.732(13), 90
***V* (Å³)**	2859.9(7)	3979(4)
Z	2	2
Radiation type	Mo *K*α (λ = 0.71073)	Mo *K*α (λ = 0.71073)
μ (mm⁻¹)	2.28	1.645
Diffractometer	Bruker *APEX*-II CCD	Bruker *APEX*-II CCD
T_{min}, T_{max}	0.411, 0.493	0.631, 0.746
No. of measured and observed [$I > 2\sigma(I)$] reflections	47998, 5647	46604, 9873
R_{int}	0.1461	0.087
$R[F^2 > 2\sigma(F^2)]$, $wR(F^2)$, S	0.0443, 0.0695, 0.958	0.0439, 0.0743, 1.016
No. of reflections	5647	9873
No. of parameters	433	542
No. of restraints	0	7
	$w = 1/[\sigma^2(F_o^2) + (0.0304P)^2]$, where $P = (F_o^2 + 2F_c^2)/3$	$w = 1/[\sigma^2(F_o^2) + (0.0428P)^2 + 3.637P]$, where $P = (F_o^2 + 2F_c^2)/3$
$\Delta\rho_{max}$, $\Delta\rho_{min}$ (e Å⁻³)	1.65, −2.00	1.75, −1.28

Lanthanide coordination number analysis (CCDC)

According to the Cambridge Crystallography Database (CSD)[13], the amount of structures of 8-coordinated Eu(III) complexes is 2961 and 9-coordinated ones is 2817, which shows, that there is no special preference for Eu(III) as well as for Gd(III) to have CN=9. This is, however, not the case for other lanthanides: the earlier lanthanide ions (from La to Sm) indeed prefer to coordinate 9 donor atoms, while heavier lanthanides (from Tb to Lu) tend to have lower coordination number of 8, which is in line with lanthanide contraction. The results of the database analysis is shown in a Figure S3, where the violin plot shows the distribution of coordination numbers of lanthanides.

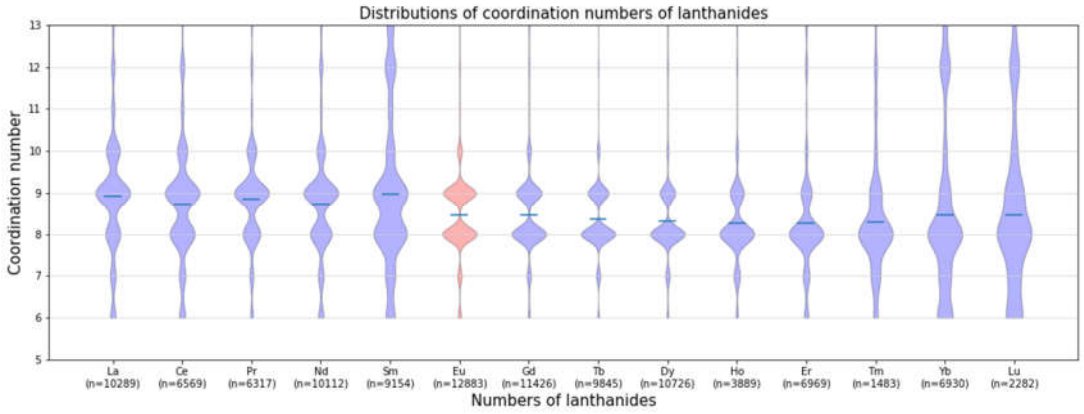

Figure S3 Distribution of Ln coordination numbers according to the CCDC analysis using violin plot. The horizontal line indicates the mean value.

Time-resolved FTIR

The time-resolved FTIR investigation of **1a** in the region between 1800 and 1000 cm^{-1} yielded strong evidence for the population of a long lived electronically excited state after excitation with a 355 nm laser pulse. Directly after excitation negative and positive absorption bands are found in the step-scan difference spectrum. Negative bands are due to ground state depopulation, which can be seen by the good correlation between negative bands in the step-scan difference spectrum and the ground state spectrum. The positive bands in the step-scan difference spectrum are due to the population of an electronically excited state and are all shifted to lower wavenumbers compared to the absorption bands of the electronic ground state vibrations with a relatively large shift of 27 cm^{-1} for most intense peaks at 1403 to 1376 cm^{-1}. The mentioned red shifts are probably due to a bond weakening in the electronic excited state, compared to the electronic ground state. In the investigated spectral region mostly C=C and C,N stretching vibrations and C-H bending and rocking vibrations are found. The experimental difference spectra show a strong change in absorbance directly after excitation of the sample followed by a slow decay of the signal intensity without shifts in the band positions; this is showing the repopulation of the electronic ground state. So far, it is assumed that only one excited electronic state is populated on our time-scale from 100 ns to 500 µs.

TD-DFT

All calculations have been performed with Gaussian 09, where the B3LYP functional with the cc-pVDZ basis set for F, C, H, N, and O and the MWB52 ECP for Eu are used. The resulting IR spectrum in the same range as the measured step-scan spectrum is shown below, the peaks are fitted with a Gaussian (FWHM=15 cm^{-1}) (Figure S4 a).

The spectrum can represent the experimental one very well. The intense first peak results from C=O stretching vibrations of the carboxylic groups. A complete table of the vibrations will be provided when a direct comparison of theory and experiment is depicted.

The absorption spectrum is calculated using TD-DFT, FWHM=2000 cm^{-1}. f-f excitation cannot be represented since the ECP contains all f electrons (Figure S4 b). The first excitation (313 nm) represents a combination of a $\pi - \pi^*$ excitation in the 1,10-phenanthroline ligand and an ILCT from the bridging fluorbenzoate to the phenanthroline. The most intense transition (295 nm) results mainly from an ILCT from the non-bridging fluorbenzoate to the phenanthroline.

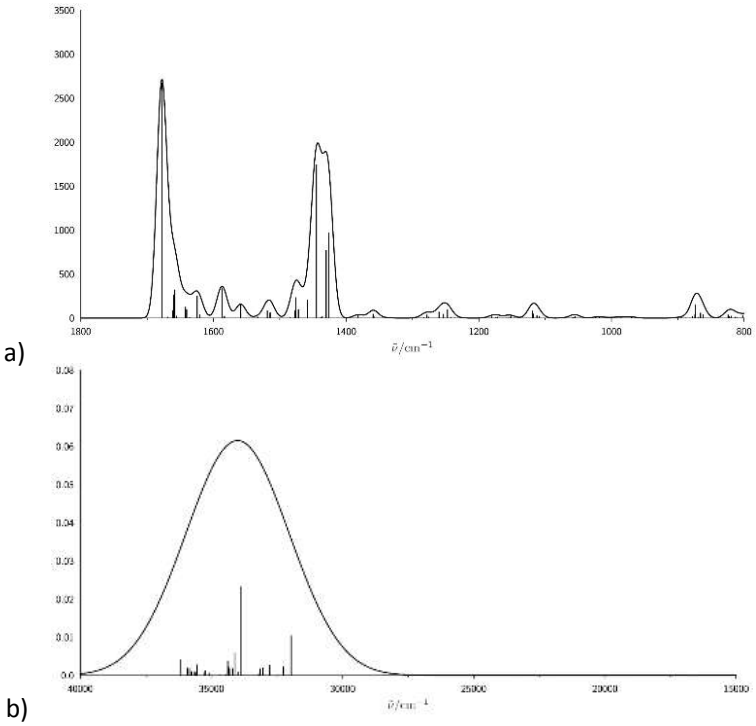

Figure S4 a) the calculated IR spectrum of **1a** b) the calculated absorption spectrum of **1a.** Both results are consistend with the experimental data.

PXRD data for the complexes within b-series

1b

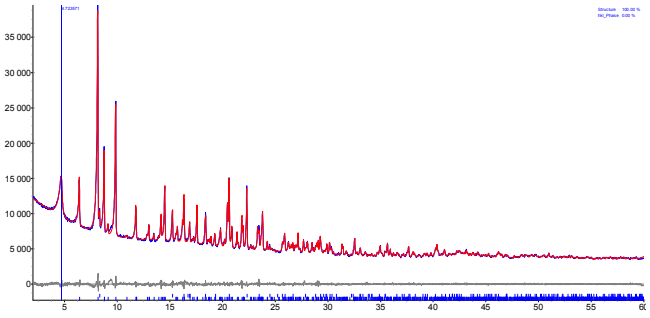

Spacegroup	P21/c
Cell Volume (Å^3)	3823.4(4)
a (Å)	15.7340(8)
b (Å)	13.5752(5)
c (Å)	20.4815(11)
beta (°)	119.076(4)

2b

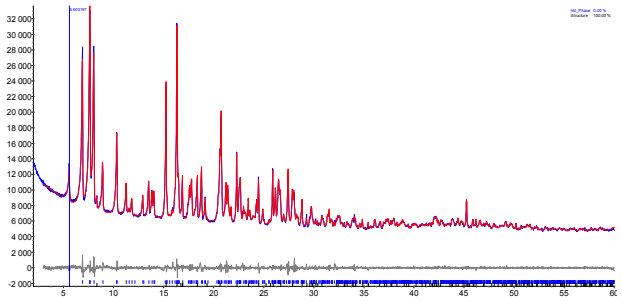

Spacegroup	P-1
Cell Volume (Å^3)	1914.9(2)
a (Å)	11.9140(8)
b (Å)	14.2836(10)
c (Å)	12.5860(9)
alpha (°)	112.469(5)
beta (°)	89.278(5)
gamma (°)	103.778(4)

3b.

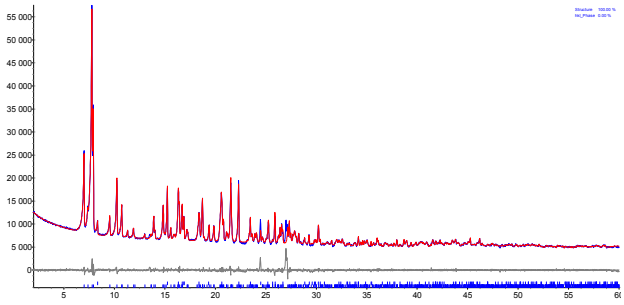

Spacegroup	P-1
Cell Volume (Å^3)	1895.7(3)
a (Å)	11.5437(9)
b (Å)	13.0522(13)
c (Å)	13.9630(12)
alpha (°)	113.568(7)
beta (°)	79.450(6)
gamma (°)	94.071(6)

Photophysical properties

The excitation and emission spectra of the powders is represented on Figure S5. All the complexes show a typical Eu-centered luminescence with sharp luminescent bands, corresponding to f-f transitions.

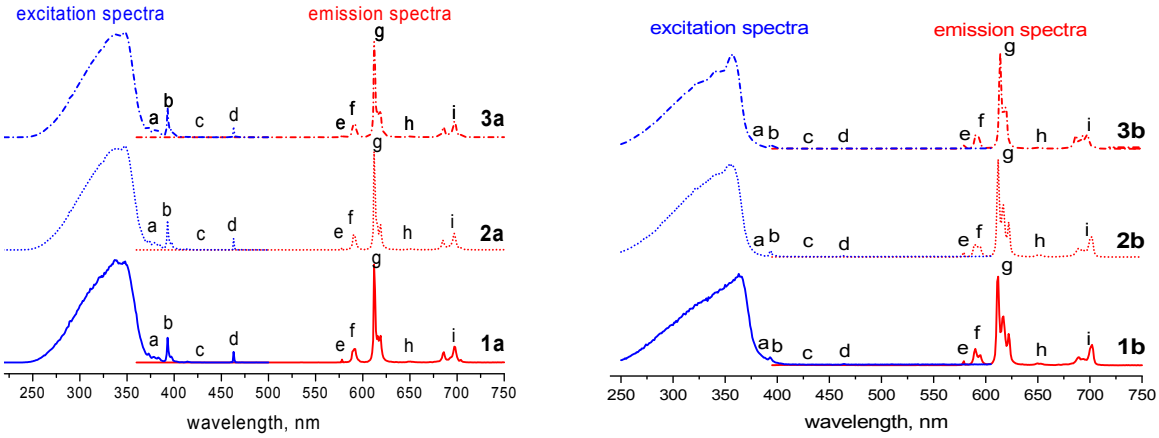

a) b)

Figure S5 Luminescence spectroscopy for Eu complexes with a) Phenanthroline (a-series) and b) Bathophenanthroline (b-series): left, blue color – excitation monitored at 612.0 nm (uncorrected spectrum); right, red color – emission excited at 347.0 nm and corrected for detector sensitivity. Peak assignment for excitation: a=$^5G_6$, $^5G_5$←$^7F_1$, b=$^5L_6$←$^7F_0$, c=$^5D_3$←$^7F_1$, d=$^5D_2$←$^7F_0$, for emission e=$^5D_0$→$^7F_0$, f=$^5D_0$→$^7F_1$, g=$^5D_0$→$^7F_2$, h=$^5D_0$→$^7F_3$, i=$^5D_0$→$^7F_4$

We measured the intrinsic quantum yields for Eu(III) complexes within a-series, because the excitation band $^5L_6$←$^7F_0$ (λ=390 nm) does not overlap with the excitation of the ligand (Figure S5a). This is, however, not the case for the complexes within b-series, for which the band λ=390 nm is hidden behind the ligand excitation.

Nevertheless, the measurements, performed for the complexes within a-series, show, that the experimental and calculated data are in a good agreement.

The luminescence in aqueous solutions was also measured for the complexes within a-series, showing the same position of luminescent bands in powders, witnessing Eu-centered luminescence (Figure S6). Luminescence in aqueous solutions was not measured for Eu complexes within b-series, due to their poor aqueous solubility.

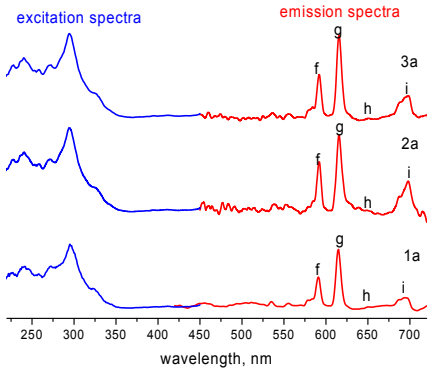

Figure S6 luminescence spectra of 0.5 mM aqueous solution of Eu complexes within a-series.

Luminescence decay profiles.

Complexes within a-series

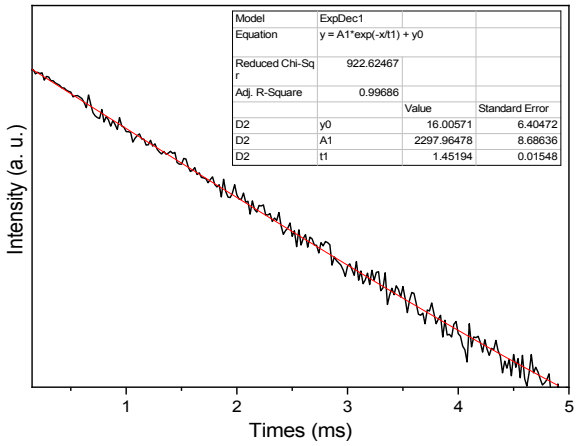

a)

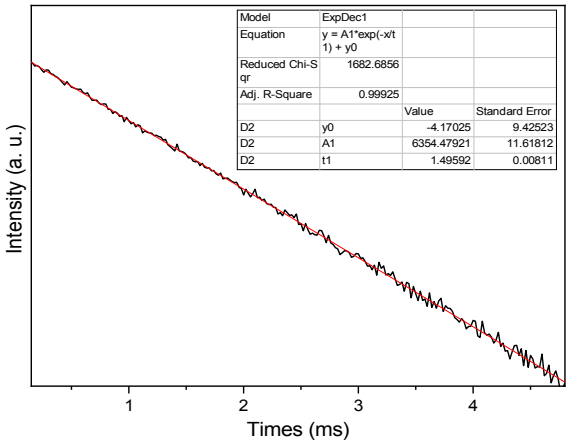

b)

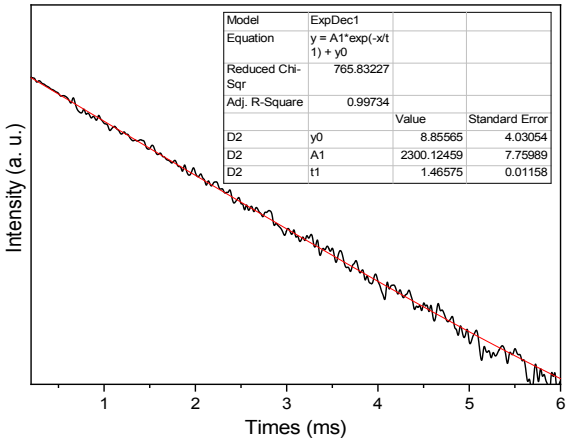

c)

Figure S7 The luminescence decay plot for the complexes within a-series: a) compound **1a**, determined lifetime 1.45 ms, b) compound **2a**, determined lifetime 1.50 ms c) compound **3a**, determined lifetime 1.46 ms

Complexes within b-series

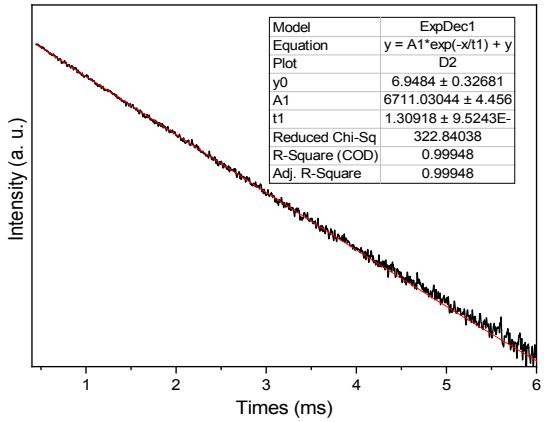

a)

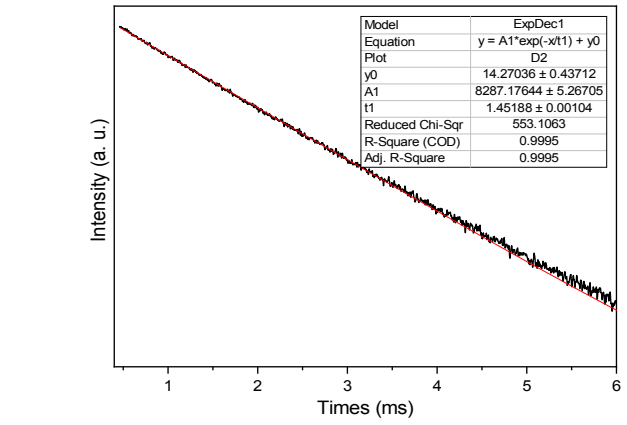

b)

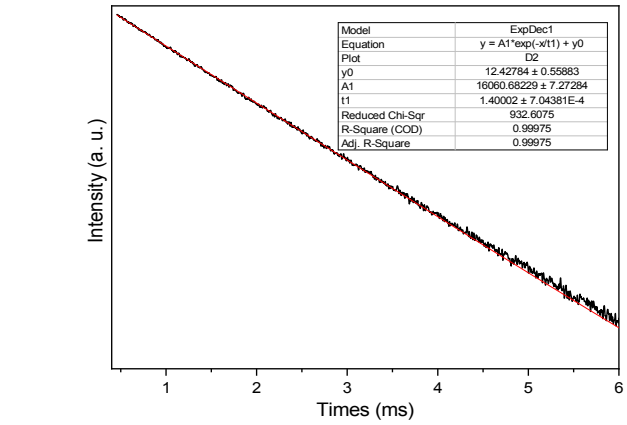

c)

Figure S8 The luminescence decay plot for the complexes within a-series: a) compound **1b**, determined lifetime 1.31 ms, b) compound **2b**, determined lifetime 1.45 ms c) compound **3a**, determined lifetime 1.40 ms

Cellular experiments:

The cellular experiments were performed using HeLa cells. Firstly, the safe concentrations of aqueous solutions of the studied compounds were determined. Due to high aqueous solubility, the complexes **1a**, **2a**, **3a** were tested in aqueous or EtOH/H_2O (1:2) solutions. Since we did not observe any significant differences by using these solvent systems, the further experiments for a-series were performed in water. The complexes within b-series turned out to be less water-soluble, that is why they were tested in DMSO/H_2O (1:4) media. The safe concentrations were determined using MTT assay and defined as the concentration of the complex in cellular media, where more than 80% are alive after 72 h of incubation with the sample. The safe concentrations turned out to be in the range 0.15 – 0.5 mM, which is quite high concentration for cellular imaging.

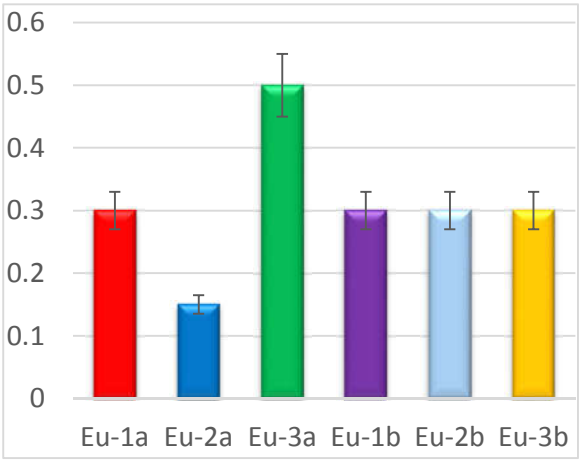

Figure S9 Safe concentrations in mM (viability of the cells is more than 80%) of the complexes, determined with MTT assay. Aqueous solutions for the complexes in a-series, DMSO/H_2O (1:4) solutions for the complexes in b-series.

The complexes at the concentrations far below the safe level were tested in HeLa cells. The complexes from 1-series showed characteristic Eu(III)-based red luminescence and were tested at different concentrations and were still luminescent even at low concentrations of 0.5 µM (Figure S10). However, the complexes from b-series with BPhen auxiliary ligand turned out to be unsatisfactory for cellular imaging and were not uptaken by cells.

a)

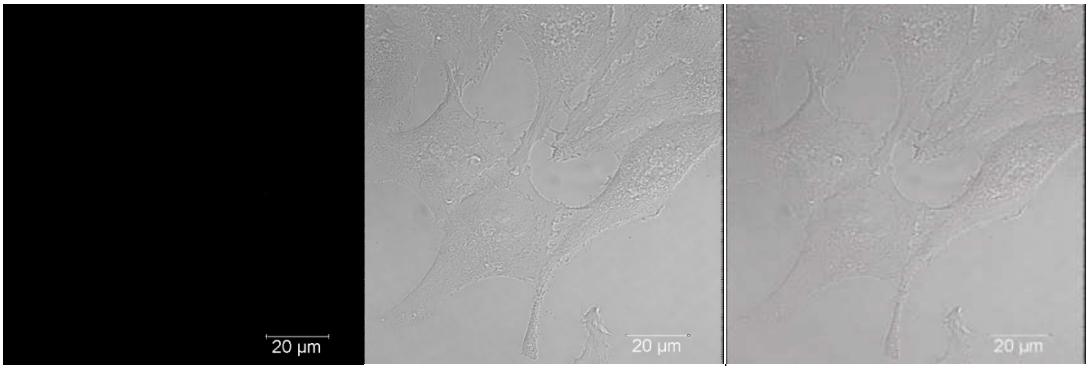

b)

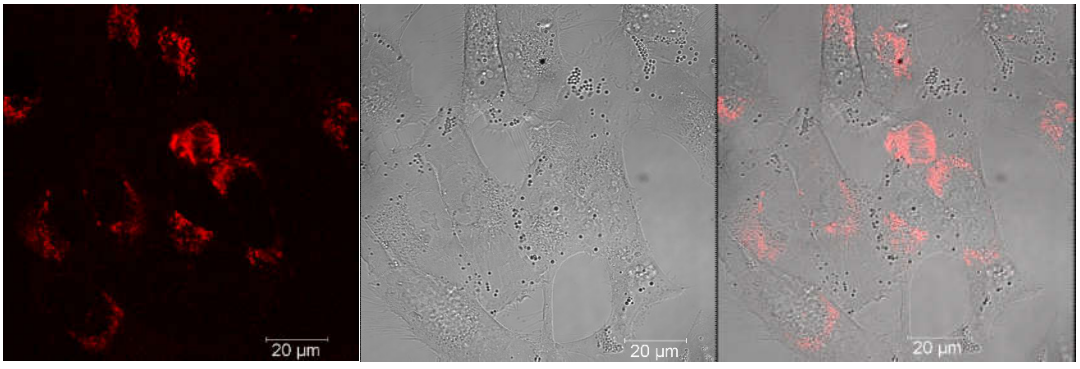

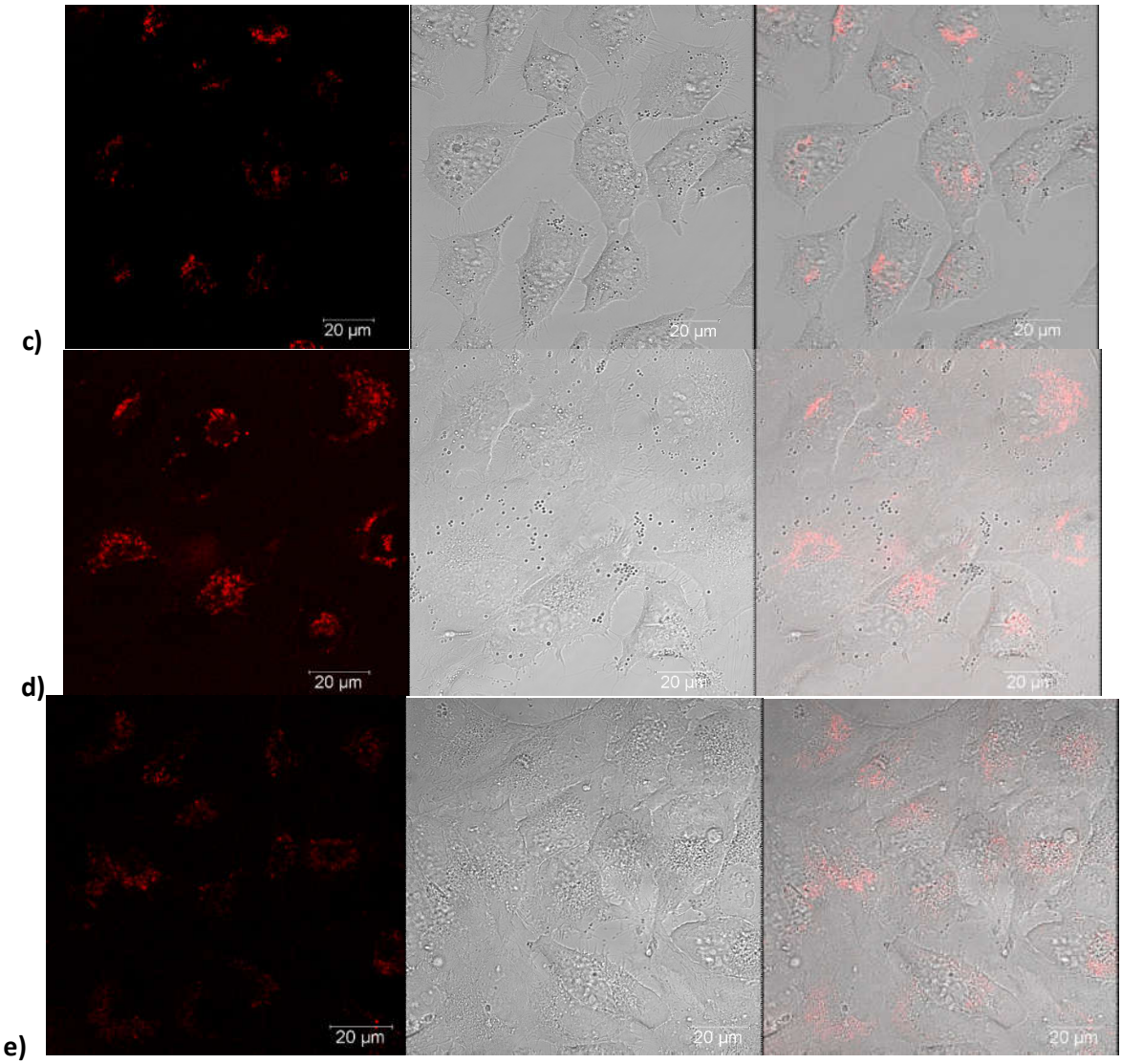

Figure S10 the confocal microscopy (laser 405 nm, power 30%) images for a) control b) **1a,** 10 µM c) **1a,** 0.5 µM d) **2a,** 10 µM e) **3a,** 0.5µM

The complexes did not show any specific localization in cells, however, they proved to be luminescent in cellular media. The further improvement may be achieved by fuctionalization of the ligands so that the specific localization in cells can be achieved (for instance, this is what is done with DOTA or DO3A-based ligands, where ligand functionalization leads to the targeting properties, see [14,15]).

In comparison to our previous research[16], where the complexes 1 - 3 were tested in cells, compounds 1a-3a are shown to be much more intensive, giving an intense luminescence at the concentration of 0.5 µM, which is 200-times lower than the lower possible concentration of compound 1, when it's luminescence is still detectable (0.1mM).

OLED manufacturing

High quantum yield of the obtained compounds makes them promising for electroluminescent applications, i.e. as an emission layer for OLEDs. For this purpose, several key properties have to be ensured additionally to the high Q_{tot}, such as 1) high absorption for high emission brightness and 2) charge transport properties, leading to the exciton formation[17–19]. To demonstrate the charge carrier mobility, most efficient complexes **1a**, **1b**, **2a, 2b** were tested in OLEDs. For the electroluminescence (EL) tests the heterostructure PEDOT:PSS/ PVK/EML/TPBi/Al was used (where EML is an emission layer).
Firstly TCs with Phen, exhibiting the highest PLQY values, were tested. In both spectra the band of europium luminescence, corresponding to $^5D_0 \rightarrow {}^7F_2$ is well-detected, however, both spectra are dominated by the broadband luminescence of transport layers (Fig. S9).

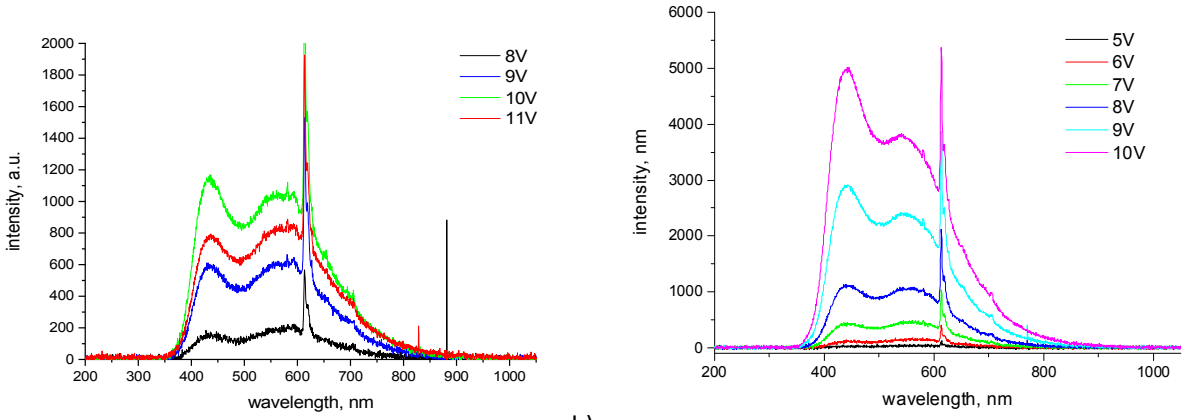

a) b)

Figure S11 EL spectra of OLED with the structure PEDOT:PSS/ PVK/EML/TPBi/Al, where a) EML = 1a and b) EML = 2a

Similar situation was observed by some of us recently[17], where the emission layer made of another Eu(III) TC doped in Phen host was used. The reason of such behaviour is insufficient electron mobility of Phen together with its too high LUMO level (1.2 eV), which serves as a blocking, rather than transport layer. Despite the use of a single-component TCs as the EML instead of the doped film, the similar behaviour is observed in the present case. Since fluorobenzoate anion does not exhibit any transport properties, charge carrier transport can only occur through the neutral ligand. The high LUMO level of Phen did not allow OLED heterostructure optimization using common electron-transport materials. Therefore, the record value of the PLQY does not result in high performance of **1a** and **2a** as emitting materials in OLEDs. Unlike this, the use of BPhen containing complexes **1b** and **2b** resulted in pure ionic Eu(III) luminescence. Given the similar structures of the complexes, almost the same IV curves of both compounds witness that indeed the neutral ligand is responsible for the charge transport

Therefore, two ligands, known for the almost the same absorption and very similar europium ion sensitization efficiency, behave very differently in complexes under electroexcitation. BPhen, known for very high electron mobility ensures efficient electroexcitation and pure and bright europium luminescence in the complexes, while Phen as the neutral ligand makes the mLC serve as a blocking layer, which thus exhibits almost no europium luminescence.

Supporting literature:

1. Coelho, A. A. & IUCr. Indexing of powder diffraction patterns by iterative use of singular value decomposition. *J. Appl. Crystallogr.* **36,** 86–95 (2003).
2. *TOPAS 4.2 User Manual*. (Bruker AXS GmbH, 2009).
3. Favre-Nicolin, V., Černý, R. & IUCr. *FOX* , `free objects for crystallography': a modular approach to *ab initio* structure determination from powder diffraction. *J. Appl. Crystallogr.* **35,** 734–743 (2002).
4. Bushmarinov, I. S., Dmitrienko, A. O., Korlyukov, A. A., Antipin, M. Y. & IUCr. Rietveld refinement and structure verification using `Morse' restraints. *J. Appl. Crystallogr.* **45,** 1187–1197 (2012).
5. Smrčok, Ľ., Jorík, V., Scholtzová, E., Milata, V. & IUCr. *Ab initio* structure determination of 5-anilinomethylene-2,2-dimethyl-1,3-dioxane-4,6-dione from laboratory powder data – a combined use of X-ray, molecular and solid-state DFT study. *Acta Crystallogr. Sect. B Struct. Sci.* **63,** 477–484 (2007).
6. Grimme, S. Semiempirical GGA-type density functional constructed with a long-range dispersion correction. *J. Comput. Chem.* **27,** 1787–1799 (2006).
7. Kresse, G. & Hafner, J. *Ab initio* molecular-dynamics simulation of the liquid-metal–amorphous-semiconductor transition in germanium. *Phys. Rev. B* **49,** 14251–14269 (1994).
8. Kresse, G. & Furthmüller, J. Efficiency of ab-initio total energy calculations for metals and semiconductors using a plane-wave basis set. *Comput. Mater. Sci.* **6,** 15–50 (1996).
9. van de Streek, J., Neumann, M. A. & IUCr. Validation of experimental molecular crystal structures with dispersion-corrected density functional theory calculations. *Acta Crystallogr. Sect. B Struct. Sci.* **66,** 544–558 (2010).
10. Li, X. & Zhang, Z.-Y. Synthesis, structure and luminescence properties of two novel lanthanide complexes with 2-fluorobenzoic acid and 1,10-phenanthroline. *J. Coord. Chem.* **59,** 1873–1882 (2006).
11. Dolomanov, O. V. *et al. OLEX2* : a complete structure solution, refinement and analysis program. *J. Appl. Crystallogr.* **42,** 339–341 (2009).
12. Sheldrick, G. M. & IUCr. A short history of *SHELX*. *Acta Crystallogr. Sect. A Found. Crystallogr.* **64,** 112–122 (2008).
13. Taylor, R. & Allen, F. H. in (eds. Bürgi, H.-B. & Dunitz, J. D.) 111–161 (Wiley-VCH Verlag GmbH, 1994).
14. Parker, D. Luminescent lanthanide sensors for pH, pO2 and selected anions. *Coord. Chem. Rev.* **205,** 109–130 (2000).
15. Butler, S. J., Lamarque, L., Pal, R. & Parker, D. EuroTracker dyes: highly emissive europium complexes as alternative organelle stains for live cell imaging. *Chem. Sci.* **5,** 1750 (2014).
16. Kalyakina, A. S. *et al.* Lanthanide Fluorobenzoates as Bio-Probes: a Quest for the Optimal Ligand Fluorination Degree. *Chem. - A Eur. J.* **23,** (2017).
17. Utochnikova, V. V. *et al.* Lanthanide tetrafluorobenzoates as emitters for OLEDs: New approach for host selection. *Org. Electron.* **44,** 85–93 (2017).
18. Utochnikova, V. V. *et al.* Lanthanide 9-anthracenate: solution processable emitters for efficient purely NIR emitting host-free OLEDs. *J. Mater. Chem. C* (2016). doi:10.1039/C6TC03586H

19. Bünzli, J. C. G., Comby, S., Chauvin, A. S. & Vandevyver, C. D. B. New Opportunities for Lanthanide Luminescence. *J. Rare Earths* **25,** 257–274 (2007).